

CentennialScale Variability of the Atlantic Meridional Overturning Circulation in CMIP6 Models Shaped by Arctic–North Atlantic Interactions and Sea Ice Biases

Original

CentennialScale Variability of the Atlantic Meridional Overturning Circulation in CMIP6 Models Shaped by Arctic–North Atlantic Interactions and Sea Ice Biases / Mehling, Oliver; Bellomo, Katinka; von Hardenberg, Jost. - In: GEOPHYSICAL RESEARCH LETTERS. - ISSN 0094-8276. - ELETTRONICO. - 51:20(2024). [10.1029/2024gl110791]

Availability:

This version is available at: 11583/2993789 since: 2024-10-28T14:39:09Z

Publisher:

American Geophysical Union

Published

DOI:10.1029/2024gl110791

Terms of use:

This article is made available under terms and conditions as specified in the corresponding bibliographic description in the repository

Publisher copyright

(Article begins on next page)

Accuracy Evaluation of On-Wafer Load–Pull Measurements

Andrea Ferrero, *Member, IEEE*, Valeria Teppati, and Alessio Carullo

Abstract—This paper investigates the residual calibration uncertainty effects in on-wafer load–pull measurements. After the systematic error correction (based on a traditional error-box model) has been applied, the residual uncertainty on absolute-power-level measurements can dramatically affect the accuracy of typical nonlinear parameters such as gain and power-added efficiency under different load conditions. The main residual uncertainty contributions are highlighted both by a theoretical analysis and experiments. Finally, one of the possible causes for intermodulation-distortion measurement errors is shown.

Index Terms—Accuracy, load–pull, microwave measurements.

I. INTRODUCTION

THE well-known load–pull measurement techniques consist of monitoring the nonlinear performances of a device-under-test (DUT) while driving it with different load impedance values. Since 15 years ago, passive and active load–pull systems have been widely used for characterizing power devices and designing power amplifiers [1]. With today’s impressive growth of wireless communications, the optimization of nonlinear performances in terms of delivered output power and especially power-added efficiency (PAE) plays a fundamental role both from an engineering and marketing point-of-view. The need of increasing the accuracy of load–pull measurements becomes a must when a few percentages of difference in PAE or an increase of a few milliwatts for the maximum output power determine the success of a design or of a new device technology. Load and source–pull calibration techniques are all based on the use of a network analyzer (NWA) to obtain the value of the reflection coefficients presented by a tuner or by an active load system. The load-setting technique could be substantially different using traditional passive tuners [2] or active systems [3], but in both cases, an NWA is used to obtain the setting impedance values. For a traditional passive system, the tuner is measured in advance with an ordinary S -parameter NWA, and then the uncertainty relies on mechanical repeatability and deembedding techniques. On the contrary, real-time NWA based load–pull systems are calibrated by means of the insertion of standards at the on-wafer reference planes [3]–[5].

The power values are obtained through the use of power meters for traditional passive systems or through a direct reading of the powers by the NWA with the real-time systems. However,

in the latter case, a calibration of the NWA in terms of absolute-power levels is mandatory [3].

For both techniques, the overall measurement uncertainty basically depends on the system capability to accurately measure power levels when high mismatched loads and high input power are set.

Although many papers deal with the systematic effect correction on both power and reflection-coefficient measurements, an extensive investigation of the residual calibration uncertainty and its effect on load–pull data was never attempted before, to the authors’ knowledge.

In this paper, we have treated the following open problems in order to achieve more accurate load–pull measurements.

- 1) Which is the residual calibration uncertainty of input power and output power (P_{in} , P_{out}), gain (G), and PAE (PAE or η)?
- 2) Which is G and PAE uncertainty for highly mismatched loads?
- 3) Which is the noise floor effect of the input amplifier [usually a traveling-wave tube amplifier (TWTA)] on the measurement uncertainty?
- 4) Which is the effect of the input-amplifier parasitic intermodulation (IM) on active-device IM measurements?

II. PROBLEM DEFINITION

In order to answer the previous questions, the authors followed the following methodology:

- sensitivity analysis of the estimated parameters (P_{in} , P_{out} , G , and PAE) with respect to the measured quantities;
- evaluation of the residual calibration uncertainty by means of especially designed experimental tests;
- estimation of the expected combined uncertainty of P_{in} , P_{out} , G , and PAE.

The proposed methodology can be applied to any passive or active load–pull measurement system, but we will concentrate on the active load–pull system shown in Fig. 1, which has the following main characteristics:

- on-wafer NWA based real time system;
- thru-reflection-line (TRL) like calibration technique for S -parameter and reflection coefficient associated with a power calibration for absolute-power-level measurements [4].

Such a system should present better accuracy compared to usual load–pull systems based on power meter because not only ratio parameters (i.e., the input and load reflection coefficients

Manuscript received April 4, 2000; revised August 25, 2000.

The authors are with the Dipartimento di Elettronica, Politecnico di Torino, 10129 Turin, Italy (e-mail: ferrero@polito.it).

Publisher Item Identifier S 0018-9480(01)01555-1.

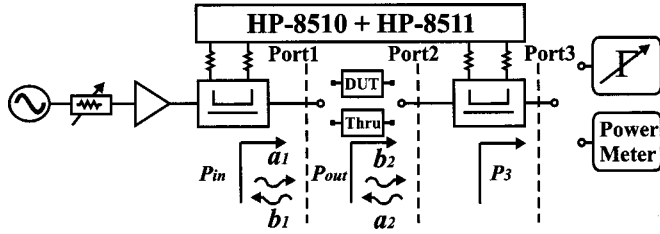


Fig. 1. Real-time load-pull system used for the estimation of the residual calibration uncertainty.

Γ_{in} and Γ_L) are measured by means of the NWA, but also absolute-power levels. This allows one a broader dynamic range and better noise immunity to be obtained with respect to the power-meter technique; furthermore, the system does not suffer from any problem related to mechanical repeatability on Γ_L setting since all the parameters are real-time measured. A power meter is also necessary in this system, but only to calibrate the absolute-power level and not during the measurements, which are completely done through the NWA. The load-setting technique can be either active or passive because the load is real-time measured.

The calibration technique, which is based on the usual error box plus a power coefficient [3], involves NWA and power meter measurements beyond the use of standards (short, open, match) connected to Port 3 and some coplanar standards connected to the probe tips. Since the contribution due to standard imperfections can be made negligible either using more precise calibration standards or using improved standard models [6], the residual calibration uncertainty can be related to the following main contributions:

- 1) NWA measurement repeatability;
- 2) incorrect power coefficient (due to power meter reading during calibration);
- 3) on-wafer probe positioning (PP) repeatability.

The unknown parameters are estimated as

$$P_{in} = |a_1|^2(1 - |\Gamma_{in}|^2) = |a_1|^2 - |b_1|^2 \quad (1)$$

$$P_{out} = |b_2|^2(1 - |\Gamma_L|^2) = |b_2|^2 - |a_2|^2 \quad (2)$$

$$G = \frac{P_{out}}{P_{in}} \quad (3)$$

$$\eta = \frac{(P_{out} - P_{in})_{Watt}}{(P_{DC})_{Watt}} \quad (4)$$

where $|a_i|$ and $|b_i|$ ($i = 1, 2$) are the incident and reflected power wave (pw) amplitudes at the input and output DUT ports (Ports 1 and 2), while P_{DC} is the dc power. The pw amplitudes are obtained from the NWA after the error coefficient deembedding, while P_{DC} is obtained from dc current and voltage measurements carried out by a six-and-one-half digits digital multimeter.

According to [7], the absolute combined standard uncertainty of the generic estimated parameter y is obtained as

$$u_c(y) = \sqrt{\sum_i c_i^2 \cdot u^2(x_i)} \quad (5)$$

where c_i are the sensitivity coefficients of y (P_{in} , P_{out} , G , or η) with respect to the input quantities x_i ($|a_1|$, $|b_1|$, $|a_2|$ or $|b_2|$) and $u(x_i)$ are their absolute standard uncertainties.

III. EXPERIMENTAL ESTIMATION OF RESIDUAL CALIBRATION UNCERTAINTY

Since we are considering on-wafer measurements and any on-wafer power meter is available, we address the problem of finding an experimental technique to highlight the contributions of the residual calibration uncertainty.

A thru standard is inserted at the on-wafer reference planes and a power meter is connected at coaxial Port 3 of the measurement system (see Fig. 1).

The calibrated values of the pw amplitude $|a_1|$, $|b_1|$, $|a_2|$, $|b_2|$ are carried out by means of the NWA and the power P_3 is measured with the power meter.

We consider now the insertion loss (IL) of the output reflectometer

$$IL = P_{in}/P_3. \quad (6)$$

Since this network is passive, its IL should be constant no matter which power levels are used; furthermore, it is well matched (i.e., loaded with the power meter); thus, the evaluation of the IL is not affected by mismatch contributions. For those reasons, the IL measurements can be employed to evaluate the residual uncertainty due to incorrect calibration power coefficient and NWA repeatability.

IL values have been estimated for different input power levels; each set of data have been measured ten times and every parameter averaged; furthermore, every NWA measurement is obtained as the average of 128 readings in order to reduce the noise effect.

The following four calibrations have been performed with two different calibration power levels:

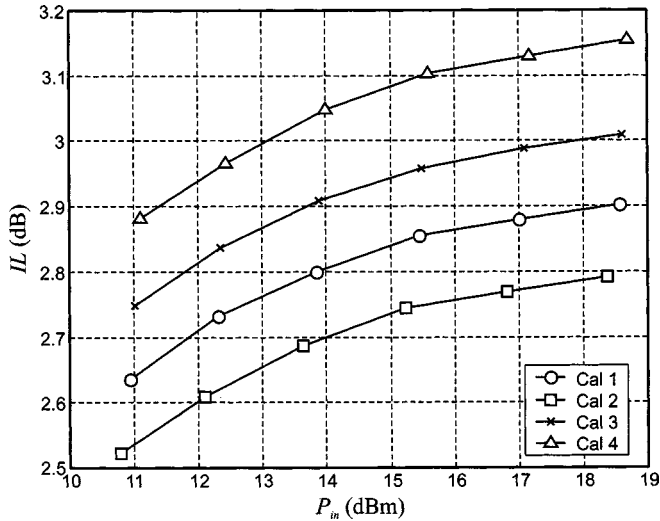
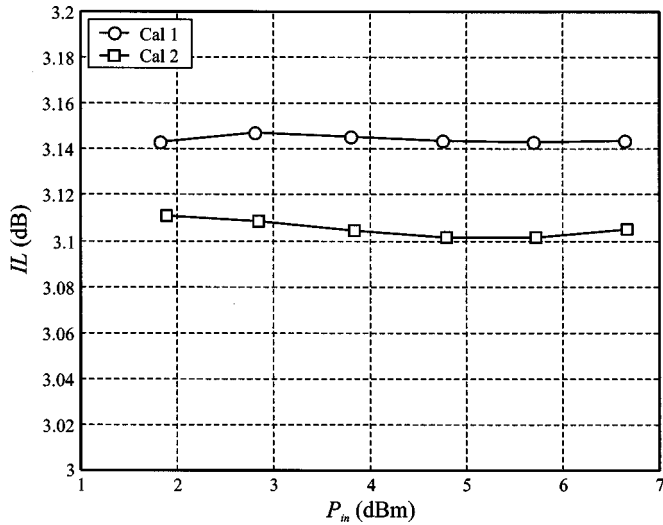
- 1) @18 GHz, 15.5 dBm;
- 2) @18 GHz, 15.5 dBm;
- 3) @18 GHz, 10.2 dBm;
- 4) @18 GHz, 10.2 dBm.

Each test consists of a set of IL measurements at different input power levels, using the four sets of calibration coefficients.

Fig. 2 shows the obtained results, which highlight a high sensitivity of IL with respect to the input power and a high deviation for the different calibrations.

The increase of IL with the input power, which is similar for every different calibration, is due to the presence of a TWTA in the system input-branch during both the calibration and the measurement phase. Such an amplifier has a high noise level, which influences both the power calibration coefficient and the power-meter readings, thus dramatically affecting the final results on power level measurements, as explained in the Appendix.

A second series of tests have been performed without the TWTA for two different calibrations, obtaining the results shown in Fig. 3. In this case, the sensitivity of IL with respect to the input power is negligible and its deviation with respect to the calibration is drastically reduced.


 Fig. 2. IL versus P_{in} for different calibrations.

 Fig. 3. IL versus P_{in} for two calibrations without a TWTA.

The pw amplitudes ($|a_1|$, $|b_1|$, $|a_2|$, and $|b_2|$) obtained from the different IL measurements give an estimate of the inter-calibration (IC) repeatability due to the incorrect power meter readings during the calibration.

The relative value of the experimental standard deviation $u_{ICr}(|pw|)$ for each pw and for the N_C calibrations given by

$$u_{ICr}(|pw|) = \frac{\sqrt{\frac{1}{N_C - 1} \sum_{j=1}^{N_C} (|pw_j| - |pw_{mean}|)^2}}{|pw_{mean}|} \quad (7)$$

has a maximum value of about 2% for the calibrations performed with the TWTA, while for the calibrations performed without a TWTA, values less than 0.5% have been obtained.

Moreover, the repeatability of the NWA can be estimated by analyzing each ten-reading data sets; the relative experimental standard deviation $u_{NWA r}(|pw|)$ due to the NWA repeatability has been evaluated to be of less than 0.1% in both calibrations cases (with and without TWTA). Such a contribution appears to

be negligible compared to the IC repeatability due to incorrect power coefficients.

The estimated NWA repeatability refers to a matched load condition (i.e., the power meter). A new series of experimental tests have been performed in order to evaluate the NWA repeatability in highly mismatched load conditions. Twenty pw sequential readings have been carried out for different calibrations and different power levels with a short coplanar standard at the probe tips (Port 1). The obtained results have shown a relative experimental standard deviation of about 0.1%, which is similar to the matched case.

Eventually, the uncertainty contribution related to the PP repeatability has been estimated by means of a series of tests performed by raising and lowering the probes. This involves only a part of the problem that causes repositioning errors because probes could be also moved horizontally, but we focused only on the problem of testing same dimension devices, which is common for automatic probing systems.

The obtained relative experimental standard deviation $u_{PP r}(|pw|)$ of any of the pw amplitudes is of less than 0.2%.

The uncertainty contributions related to power coefficient, NWA, and PP repeatability can, hence, be combined in order to obtain the relative residual calibration uncertainty of the pw amplitude

$$u_r(|pw|) = \sqrt{u_{ICr}^2(|pw|) + u_{NWA r}^2(|pw|) + u_{PP r}^2(|pw|)} \quad (8)$$

whose value is of about 2% for calibrations performed with a TWTA in the system input branch and of about 0.55% without a TWTA.

IV. COMBINED UNCERTAINTY OF THE ESTIMATED PARAMETERS

The combined relative uncertainties of P_{in} , P_{out} , G , and η , which are obtained by means of (5), have the following expressions:

$$u_{cr}(P_{in}) = 2 \cdot u_r(|pw|) \cdot \frac{\sqrt{1 + |\Gamma_{in}|^4}}{1 - |\Gamma_{in}|^2} \quad (9)$$

$$u_{cr}(P_{out}) = 2 \cdot u_r(|pw|) \cdot \frac{\sqrt{1 + |\Gamma_L|^4}}{1 - |\Gamma_L|^2} \quad (10)$$

$$u_{cr}(G) = 2 \cdot u_r(|pw|) \cdot \sqrt{\frac{1 + |\Gamma_{in}|^4}{(1 - |\Gamma_{in}|^2)^2} + \frac{1 + |\Gamma_L|^4}{(1 - |\Gamma_L|^2)^2}} \quad (11)$$

$$u_{cr}(\eta) = \frac{\sqrt{P_{in}^2 \cdot u_{cr}^2(P_{in}) + P_{out}^2 \cdot u_{cr}^2(P_{out})}}{P_{in} - P_{out}} \quad (12)$$

Fig. 4 shows the relative standard uncertainty of P_{out} versus $|\Gamma_L|$: the continuous line refers to calibrations performed with a TWTA, while the dashed line refers to calibrations without a TWTA. One should note that, in both cases, the combined uncertainty is mainly due to the inter-calibration (IC) repeatability and that the output power uncertainty dramatically increases with $|\Gamma_L|$. For values of $|\Gamma_L|$ close to 0.9, the relative standard uncertainty of P_{out} can reach up to 27% in the first case and up to 7% in the second case.

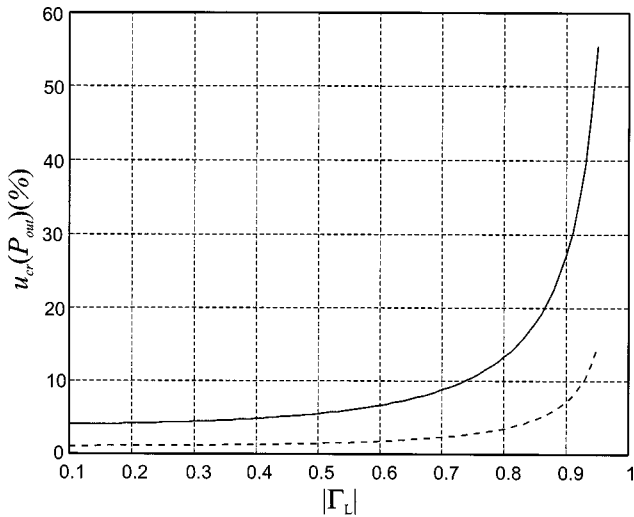


Fig. 4. Relative P_{out} standard uncertainty versus $|\Gamma_L|$ for calibrations with (continuous line) and without (dashed line) a TWTA.

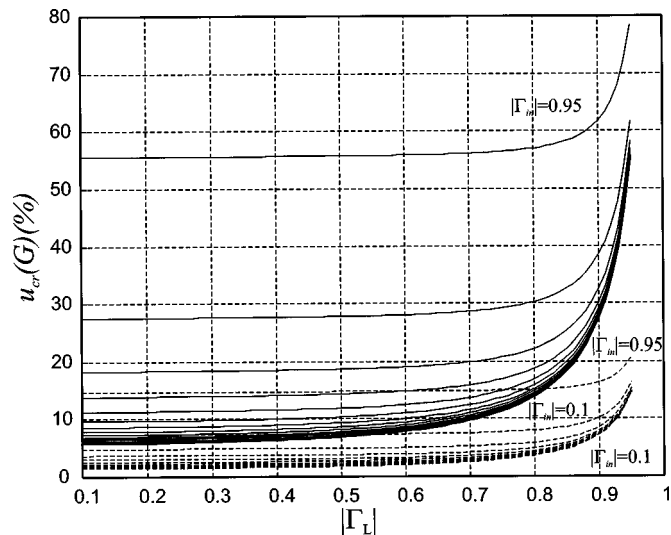


Fig. 5. Relative gain standard uncertainty versus $|\Gamma_L|$ for $|\Gamma_{\text{in}}|$ in the range of 0.1–0.95 (dashed lines refer to calibrations performed without a TWTA).

A high sensitivity of the relative standard uncertainty of G with respect to both $|\Gamma_L|$ and $|\Gamma_{\text{in}}|$ can also be seen in Fig. 5, where the uncertainties are plotted for $|\Gamma_{\text{in}}|$ in the range of 0.1–0.95. The worst uncertainty, which corresponds to $|\Gamma_L|$ and $|\Gamma_{\text{in}}|$ values close to one, is of about 78% for calibrations with a TWTA and of about 20% for calibrations without a TWTA.

The relative standard uncertainty of η , obtained by (12) for P_{in} and P_{out} values that are typical of high electron-mobility transistor (HEMT) ($P_{\text{in}} = 15.5$ dBm, $P_{\text{out}} = 25.5$ dBm), has the behavior shown in Fig. 6. In this case, the uncertainty sensitivity with respect to $|\Gamma_{\text{in}}|$ is negligible and the uncertainty value for $|\Gamma_L| = 0.95$ is of about 60% and 17% for calibrations with and without a TWTA, respectively.

The obtained results highlighted the difficult to obtain accurate measurement of parameters that are usually employed to characterize active devices in highly mismatched conditions. In this case, relative uncertainties less than 20% can be obtained only if the measurement system does not embed a TWTA in the input branch during the calibration. This condition is not always

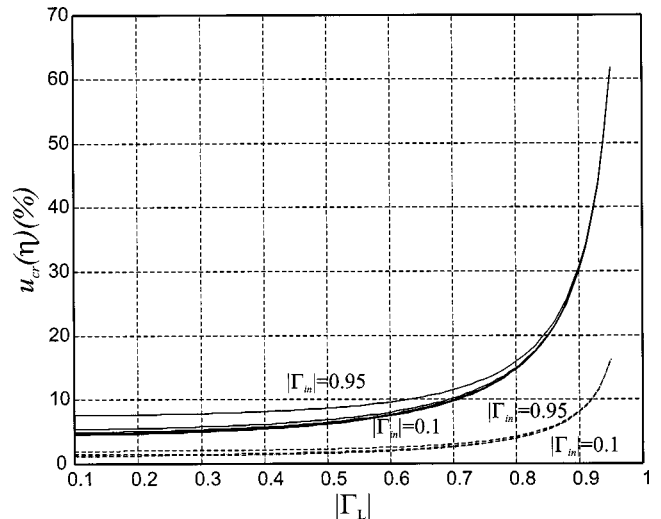


Fig. 6. Relative η standard uncertainty versus $|\Gamma_L|$ for $|\Gamma_{\text{in}}|$ in the range of 0.1–0.95 (dashed lines refer to calibrations performed without a TWTA).

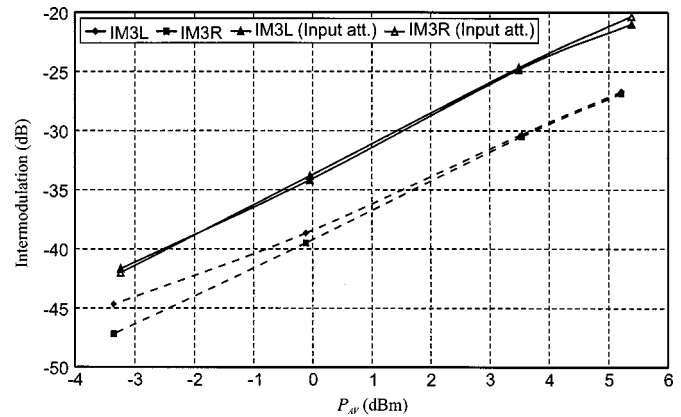


Fig. 7. Comparison of third-order IM measurements with (continuous lines) and without (dashed lines) a 20-dB attenuator at the input.

possible when millimeter-wave load-pull measurements are required. Since passive load-pull systems normally use power meters during the measurement phase, the same influence of TWT noise on the DUT parameter accuracy could be expected.

V. INPUT AMPLIFIER IM EFFECT

The effect of the input amplifier distortion on the IM measurements has been evaluated, with a measurement setup as described in [8]. This effect is particularly important when IM levels in the linear region of the device performances are considered, i.e., @8 or 10 dB of output power backoff, which is a typical requirement for highly linear power amplifiers usually employed in communication systems.

A series of experimental tests have been performed by measuring the third-order left- and right-hand-side intermodulation power levels (IM3L and IM3R, respectively) of an HEMT.

With the aim to highlight the IM3L and IM3R increasing due to parasitic contributions of the input amplifier, we have performed two different tests. The first one keeps the input IM levels below -50 dBc¹ for the maximum available power

¹dBc = dB referred to carrier power

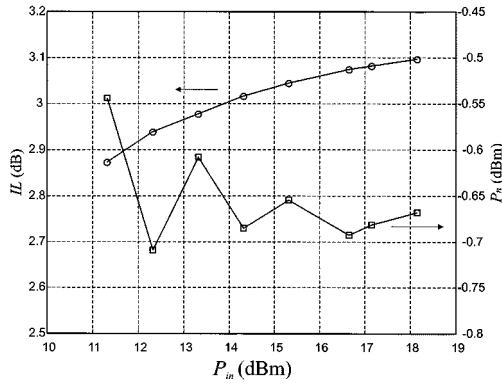


Fig. 8. Simulated IL (left-hand-side scale) and measured noise power (right-hand-side scale) for different power levels P_{in} .

(P_{AV}). In this condition, the obtained results (Fig. 7) show a maximum FET IM level of less than -25 dBc. In the second one, we put a 20-dB attenuator at the amplifier output keeping the same available power levels at the probe tips, thus obtaining a parasitic IM levels of -25 dBc at the FET input. In this condition, the maximum FET IM level is of about -20 dBc.

VI. CONCLUSIONS

In this paper, we have presented a preliminary evaluation of on-wafer load-pull measurement uncertainty for gain, PAE, and on-wafer power levels.

The obtained results have shown a strong influence of the input power amplifier noise on all the measurement data and the need for an extremely accurate pw measurement to minimize the residual calibration uncertainty when highly mismatched devices are measured.

The effect of the input amplifier distortion on IM measurement has been also measured for a specific case.

Further investigation will include the uncertainty contributions due to the calibration standards.

APPENDIX

To highlight the TWTA noise effects on IL, a direct measurement of the amplifier output signals with a spectrum analyzer was made. The carrier signal is 18 GHz and the analyzer frequency span is from 6 to 19 GHz (amplifier bandwidth from 8 to 18 GHz).

We integrated the noise spectrum for different carrier signal levels (carrier power P_c) and found an almost constant output noise power (P_n) of (-0.65 ± 0.12) dBm.

We assume the power meter measures the entire spectrum, i.e., $P_n + P_c$, while the NWA measures only P_c .

When computing the IL (see Fig. 1), P_{in} is obtained from the NWA, thus, $P_{in} = P_c$, while P_3 is measured with a power meter, thus, $P_3 = (P_c + P_n)/IL_{id}$, where IL_{id} is the IL of the output reflectometer for the ideal case (i.e., no noise). IL_{id} is assumed constant, ≈ 3 dB as obtained from the experiments without the TWTA.

Using the IL definition (6)

$$IL = \frac{P_{in}}{P_{in} + P_n} \cdot IL_{id}. \tag{A.1}$$

Fig. 8 shows the plot versus P_{in} of the IL computed with (A.1) by substitution of the measured noise power (P_n), which is also shown in this same figure.

We can see that the IL raises with input power (similarly to Fig. 2), and this is due to the amplifier noise.

This result confirms the hypothesis of the input amplifier noise being the main cause of errors during the calibration procedure.

REFERENCES

- [1] J. M. Cusak, S. M. Perlow, and B. S. Perlman, "Automatic load contour mapping for microwave power transistors," *IEEE Trans. Microwave Theory Tech.*, vol. MTT-22, pp. 1146–1152, Dec. 1974.
- [2] F. Sechi *et al.*, "A computer controlled microwave tuner for automated load pull," *RCA Rev.*, vol. 44, pp. 566–572, Dec. 1983.
- [3] A. Ferrero and U. Pisani, "An improved calibration technique for on-wafer large signal transistor characterization," *IEEE Trans. Microwave Theory Tech.*, vol. 42, pp. 360–364, Apr. 1993.
- [4] A. Ferrero and U. Pisani, "A unified algorithm for scattering and load pull measurement," in *IEEE Instrum. Meas. Technol. Conf.*, Brussels, Belgium, June 1996, pp. 1250–1253.
- [5] I. Hecht, "Improved error correction technique for large signal load-pull measurements," *IEEE Trans. Microwave Theory Tech.*, vol. MTT-35, pp. 1060–1062, Mar. 1987.
- [6] R. B. Marks, "A multiline method of network analyzer calibration," *IEEE Trans. Microwave Theory Tech.*, vol. 39, pp. 1205–1215, July 1991.
- [7] *ISO Guide to the Expression of Uncertainty in Measurement*, ISO, 1995.
- [8] M. Demmler, B. Hughes, and A. Cognata, "A 0.5–50 GHz on-wafer, intermodulation, load-pull and power measurement system," in *IEEE MTT-S Int. Microwave Symp. Dig.*, vol. 3, 1995, pp. 1041–1044.

Andrea Ferrero (S'85–M'85), photograph and biography not available at time of publication.

Valeria Teppati, photograph and biography not available at time of publication.

Alessio Carullo, photograph and biography not available at time of publication.